



THE UNIVERSITY *of* EDINBURGH

Edinburgh Research Explorer

Catechols and 3-hydroxypyridones as inhibitors of the DNA repair complex ERCC1- XPF

Citation for published version:

Chapman, TM, Gillen, KJ, Wallace, C, Lee, MT, Bakrania, P, Khurana, P, Coombs, PJ, Stennett, L, Fox, S, Bureau, EA, Brownlees, J, Melton, D & Saxty, B 2015, 'Catechols and 3-hydroxypyridones as inhibitors of the DNA repair complex ERCC1- XPF', *Bioorganic & Medicinal Chemistry Letters*.
<https://doi.org/doi:10.1016/j.bmcl.2015.08.031>

Digital Object Identifier (DOI):

[doi:10.1016/j.bmcl.2015.08.031](https://doi.org/doi:10.1016/j.bmcl.2015.08.031)

Link:

[Link to publication record in Edinburgh Research Explorer](#)

Document Version:

Peer reviewed version

Published In:

Bioorganic & Medicinal Chemistry Letters

Publisher Rights Statement:

This is the author's final manuscript as accepted for publication

General rights

Copyright for the publications made accessible via the Edinburgh Research Explorer is retained by the author(s) and / or other copyright owners and it is a condition of accessing these publications that users recognise and abide by the legal requirements associated with these rights.

Take down policy

The University of Edinburgh has made every reasonable effort to ensure that Edinburgh Research Explorer content complies with UK legislation. If you believe that the public display of this file breaches copyright please contact openaccess@ed.ac.uk providing details, and we will remove access to the work immediately and investigate your claim.



Catechols and 3-hydroxypyridones as inhibitors of the DNA repair complex ERCC1-XPF

Timothy M. Chapman,^{a,*} Kevin J. Gillen,^a Claire Wallace,^a Maximillian T. Lee,^a Preeti Bakrania,^a Puneet Khurana,^a Peter J. Coombs,^a Laura Stennett,^a Simon Fox,^a Emilie A. Bureau,^a Janet Brownlees,^a David W. Melton,^b Barbara Saxty^a

^a Centre for Therapeutics Discovery, MRC Technology, 1-3 Burtonhole Lane, Mill Hill, London NW7 1AD, UK

^b MRC Institute of Genetics and Molecular Medicine, University of Edinburgh, MRC Human Genetics Unit, Western General Hospital, Crewe Road, Edinburgh EH4 2XU, UK

Abstract:

Catechol-based inhibitors of ERCC1-XPF endonuclease activity were identified from a high-throughput screen. Exploration of the structure-activity relationships within this series yielded compound **13**, which displayed an ERCC1-XPF IC₅₀ of 0.6 μ M, high selectivity against FEN-1 and DNase I and activity in nucleotide excision repair, cisplatin enhancement and γ H2AX assays in A375 melanoma cells. Screening of fragments as potential alternatives to the catechol group revealed that 3-hydroxypyridones are able to inhibit ERCC1-XPF with high ligand efficiency, and elaboration of the hit gave compounds **36** and **37** which showed promising ERCC1-XPF IC₅₀ values of <10 μ M.

Keywords:

DNA repair
ERCC1-XPF
Catechol
3-Hydroxypyridone
Cisplatin potentiation

Platinum-based chemotherapeutics such as cisplatin result in several forms of DNA damage, however their effectiveness can be limited by efficient DNA repair processes. The ERCC1-XPF complex, formed from the heterodimerization of excision-repair cross complementation group 1 (ERCC1) and xeroderma pigmentosum F (XPF), has structure-specific endonuclease activity and plays an essential role in the removal of platinum-DNA adducts by nucleotide excision repair (NER).¹ It is also involved in interstrand crosslink repair (ICR) and there is evidence that it is a good target for intervention in melanoma, ovarian, lung and other cancers.¹ Inhibition of ERCC1-XPF activity therefore represents an approach to potentially enhance the effectiveness of chemotherapeutic agents such as cisplatin, however very few inhibitors have been reported in the literature.²

We sought to identify novel inhibitors of ERCC1-XPF using a high-throughput fluorescence-based *in vitro* endonuclease assay³ and one of the hits obtained was compound **1** (Figure 1) with an IC₅₀ value of approximately 30 μ M and modest ligand efficiency. The catechol motif is present in known nuclease inhibitors⁴ and although the dibromo-substitution and hydrazone motif were considered undesirable, **1** showed good selectivity for ERCC1-XPF in counter-screen assays against the nucleases FEN-1 and DNase I.³ We therefore sought to explore whether it was possible to design out the unwanted features and gain additional potency while retaining good selectivity for ERCC1-XPF. Testing of initial analogues showed that the

catechol group was required for inhibitory activity since mono- or di-methylation led to complete loss of activity. Catechols are known to be effective binders of metal ions, in particular magnesium and manganese; the activity of ERCC1-XPF is metal-dependent and the presence of Mn^{2+} is required for substrate turnover in the biochemical assay. It was therefore our hypothesis that they could inhibit ERCC1-XPF via binding to a metal ion at the endonuclease active site.

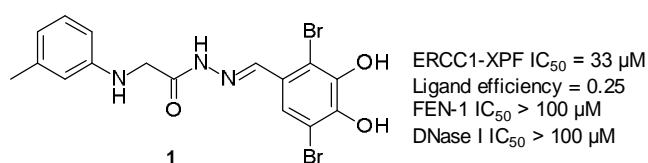


Figure 1. Initial hit compound **1**

Synthesis and testing of early analogues showed that the removal of the two bromine atoms and methyl group (Table 1, compound **2**) and replacing the hydrazono with an amide (**3**) were all well tolerated, and this led to an improvement in potency and ligand efficiency while retaining selectivity against FEN-1 and DNase I. Variation of the linker lengths on the right-hand-side portion of the amide core suggested that benzyl was preferred (**4**).

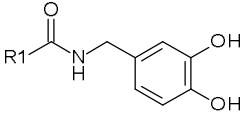
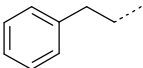
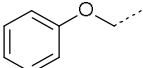
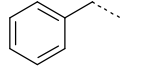
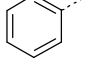
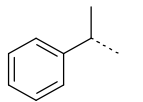
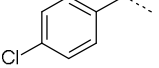
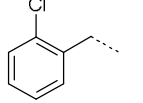
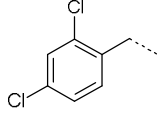
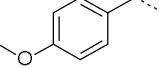
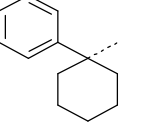
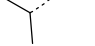
Table 1. Activity and selectivity data from analogues of initial hit

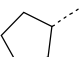
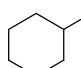
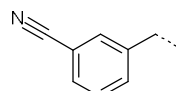
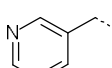
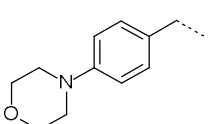
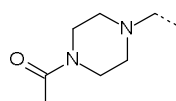
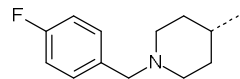
Compound	Structure	ERCC1-XPF IC_{50} / μM	FEN-1 IC_{50} / μM	DNase I IC_{50} / μM
2		2.0	>100	>100
3		15.2	>100	>100
4		0.9	>100	>100
5		1.6	>100	>100

With the benzylic catechol in place, a range of groups on the left-hand side portion of the molecule were explored (Table 2), with synthetic access through amide coupling. Replacing the aniline NH in **4** with carbon (**6**) or oxygen (**7**) both led to reductions in potency, and shortening the linker also led to losses in potency (**8**, **9**). However, the introduction of additional substituents allowed potency to be regained, such as methyl (**10**), 4-chloro (**11**) or 2-chloro (**12**). The 2,4-dichloro variant (**13**) was the most potent compound at 0.6 μM . The 4-methoxy compound (**14**) was less potent than the 4-chloro, and the larger cyclohexyl

variant (**15**) was relatively well tolerated. Smaller alkyl groups such as isopropyl (**16**) and cyclopentyl (**17**) were weak, although the cyclohexylmethyl (**18**) displayed an IC₅₀ value of just over 1 micromolar. The introduction of more polar or larger groups (**19-23**) did not lead to potency improvements relative to **13**.

Table 2. Activity and selectivity data from left-hand side variations

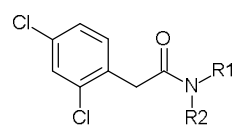
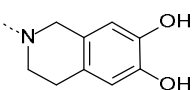
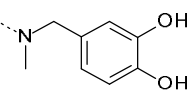
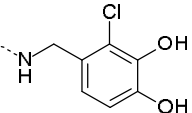
				
Compound	R1	ERCC1-XPF IC ₅₀ / μM	FEN-1 IC ₅₀ / μM ^a	DNase I IC ₅₀ / μM ^a
6		7.3	>100	>100
7		12.1	>100	>100
8		13.3	>100	>100
9		24.5	>100	>100
10		1.8	>100	nt
11		1.0	>100	>100
12		0.80	>100	>100
13		0.63	>100	>100
14		2.6	nt	nt
15		1.6	>100	nt
16		24.0	nt	nt

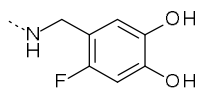
17		24.6	>100	>100
18		1.4	>100	>100
19		4.0	nt	nt
20		25.6	nt	nt
21		7.9	>100	>100
22		>100	nt	>100
23		5.8	>100	>100

^a nt = not tested.

Modifications to the right-hand side portion were explored (Table 3) via amide coupling with the 2,4-dichlorobenzyl group fixed: cyclisation (**24**) or *N*-methylation of the amide (**25**) did not significantly affect potency. Halogen substituents were added to the catechol ring to explore the effect of modifying the steric and electronic properties (**26**, **27**) including tuning the pK_a of the catechol OH groups, and although this was tolerated it did not improve potency.

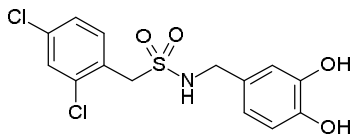
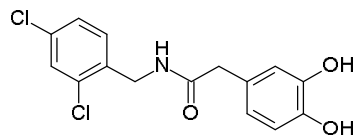
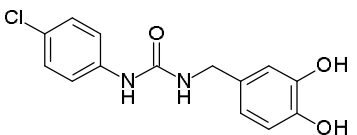
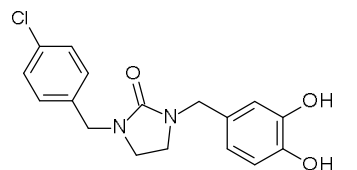
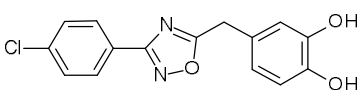
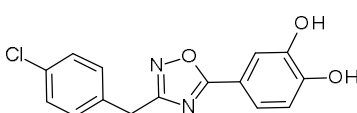
Table 3. Activity and selectivity data from right-hand side variations

				
Compound	NR1R2	ERCC1-XPF IC ₅₀ / μM	FEN-1 IC ₅₀ / μM	DNase I IC ₅₀ / μM
24		1.0	>100	>100
25		0.8	>100	>100
26		1.6	>100	>100

27		1.1	>100	>100
-----------	---	-----	------	------

Alterations to the amide core were investigated (Table 4): the sulfonamide **28** showed reduced potency in comparison with **13**, whereas the reverse amide **29** was equipotent to the parent amide. The ureas (**30**, **31**) and oxadiazole variants (**32**, **33**) also showed weaker potency compared to **13**.

Table 4. Activity and selectivity data from variations to amide core

Compound	Structure	ERCC1-XPF IC ₅₀ / μM	FEN-1 IC ₅₀ / μM	DNase I IC ₅₀ / μM
28		2.9	>100	>100
29		0.74	>100	>100
30		4.8	>100	>100
31		4.1	>100	>100
32		12.2	>100	>100
33		7.8	>100	>100

Next, the potential for modifying the catechol motif was explored; as the catechol represents a liability, especially with respect to oxidation, replacement was desirable. Previous data suggested that it would be necessary for an alternative group to have good metal-binding capability, so in order to identify catechol variants we screened a number of fragments with metal-binding capability in our biochemical assay, with the intention that these could then be merged with the existing left-hand side portion. This identified 5-bromo-3-hydroxypyridone **34** as a fragment with a promising IC₅₀ of 24 μM and high ligand efficiency (Figure 2); this fragment has recently been shown to inhibit the activity of an influenza endonuclease with a similar level of potency and bind through a metal-based interaction.^{5,6}

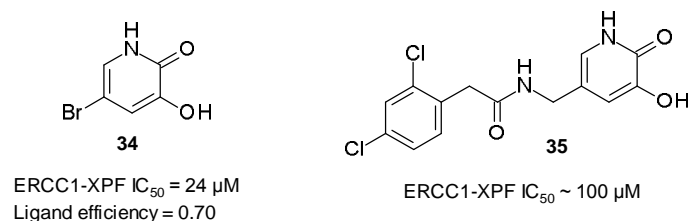
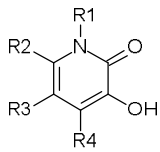
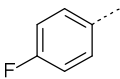
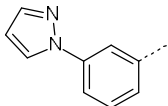
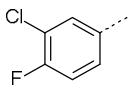
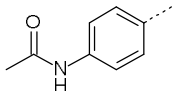
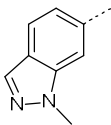
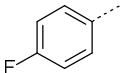
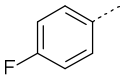
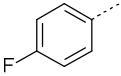


Figure 2. 5-Bromo-3-hydroxypyridone fragment **34** and merged compound **35**

However, when it was merged with the left-hand side portion of compound **13** to give **35**, this compound showed very weak activity against ERCC1-XPF, suggesting that the fragment might be binding in a different way to the catechol. Instead we therefore sought to exploit the fragment by substituting at the available positions, and due to the relative lack of structural knowledge around the protein binding site a systematic approach was employed. Firstly, replacing the bromine with a 4-fluorophenyl group (Table 5, **36**) gave a gain in potency to less than 10 μM and the 3-pyrazole substituted variant **37** showed an IC₅₀ of approximately 5 μM. A wider range of R3 variants were investigated and selected examples are shown in Table 5; although none showed improved potency compared to **37**, three other variants were within 3-fold (**38-40**). Substitution at the alternative vectors R1, R2 or R4 appeared to be poorly tolerated (**41-43**).

Table 5. Activity and selectivity data from 3-hydroxypyridone fragment substitution

<div style="text-align: center;">  </div>							
Compound	R1	R2	R3	R4	ERCC1-XPF IC ₅₀ / μM	FEN-1 IC ₅₀ / μM ^a	DNase I IC ₅₀ / μM ^a
36	H	H		H	8.7	>100	>100
37	H	H		H	5.2	>100	>100
38	H	H		H	13.1	>100	>100
39	H	H		H	13.5	>100	>100
40	H	H		H	14.6	>100	>100
41	Me	H		H	>100	nt	nt

42	H		H	H	55.2	nt	nt
43	H	H	H		>100	nt	nt

^a nt = not tested.

Compounds **13** and **36** were profiled in ADMET assays (Figure 3). Compound **13** showed relatively short mouse and human microsomal half-lives and acceptable permeability, whereas **36** showed a long half-life; both compounds were not toxic to Hep-G2 cells up to a compound concentration of 10 μ M.

Compound	Log D	Cytotox Hep-G2 v-50/ μ M	MLM $t_{1/2}$ / mins	HLM $t_{1/2}$ / mins	PAMPA P_{app} / nms^{-1}
13	2.7	>10	23	28	39
36	2.0	>10	>400	>400	44

Figure 3. Measured *in vitro* ADMET profiles for compounds **13** and **36**

Although the catechols and hydroxypyridones showed selectivity for ERCC1-XPF over FEN-1 and DNase I, catechols in particular can show PAINS effects^{7,8} and interfere with assays through non-specific mechanisms; therefore it was important to demonstrate binding to target using a biophysical method. The interaction of compounds **13** and **36** with ERCC1-XPF was examined by surface plasmon resonance (SPR). Compound **13** showed a K_D of ~ 30 μ M, weaker than the biochemical IC_{50} , with relatively slow binding kinetics (Figure 4). By contrast, the hydroxypyridone **36** showed fast binding kinetics and a K_D of 3.5 μ M, in good agreement with the biochemical IC_{50} . Neither compound showed binding to a control protein included in the study.

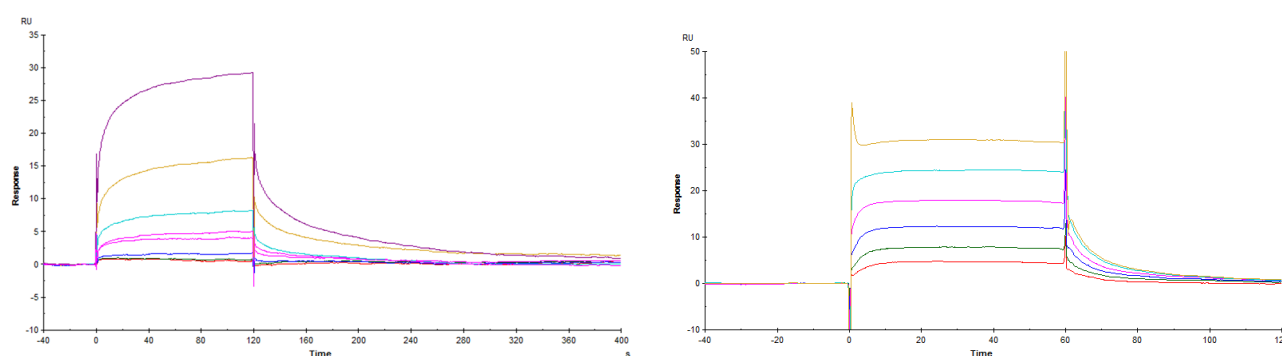


Figure 4. SPR sensorgrams for compounds **13** (left) and **36** (right)

Compound **13** was profiled in three cell-based assays using A375 melanoma cells to measure 1) direct nucleotide excision repair (NER) using a recombinant GFP reporter assay,^{3,9} 2) potentiation of cisplatin induced cell toxicity¹⁰ and 3) immunofluorescence detection of γ H2AX, a marker of DNA damage.¹¹

Firstly, in the NER assay, repair of UV damaged pEGFP plasmid was monitored following treatment with compound for 24 hours at concentrations of up to 60 μM . Compound **13** showed inhibition of NER with an IC_{50} of 15.6 μM (Figure 5).⁹

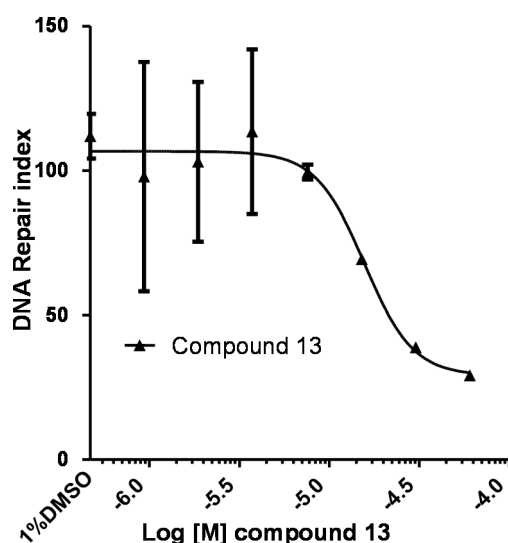
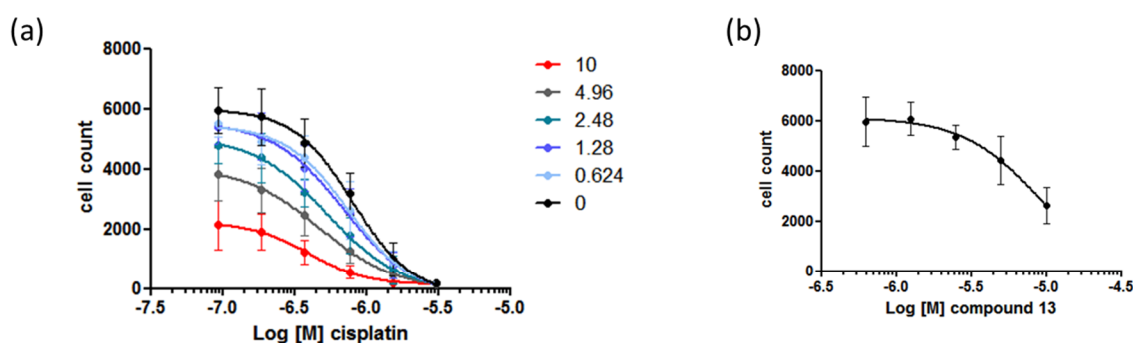


Figure 5. Compound **13** NER in A375 melanoma cell line transfected with UV damaged pEGFP and a luciferase reporter plasmid (pGL3) to control for transfection efficiency. The fluorescence read out generated as the pEGFP plasmid is repaired is normalized to both luciferase levels and readings for undamaged DNA to generate the DNA Repair Index. Inhibition of NER is detected at higher concentrations of compound, IC_{50} =15.6 μM .

Secondly, compound **13** was profiled in a cisplatin combination assay¹⁰ (Figure 6a). The compound alone showed a reduction in cell number at 4.96 and 10 μM (Figure 6b), however at compound concentrations where no toxicity was observed with compound only, there was an enhancement of cisplatin activity up to 1.5-fold (PF_{50}) as shown in the table in Figure 6.



Compound 13 (μM)	0	0.624	1.28	2.48	4.96	10
IC_{50} (μM)	0.81	0.74	0.70	0.53	0.48	0.40
PF_{50}	1	1.08	1.15	1.51	1.68	2.03

Figure 6. Cisplatin potentiation assay dose-response curves for compound **13**. A375 cells were treated in 96-well plates and cell count measured using an InCell 2000 high content imager (GE Healthcare). Curves show activity of cisplatin alone (0 μM compound) and then in combination with the indicated concentrations of compound. A shift in cisplatin potency was observed with increasing concentration of compound up to 2.03-fold

with 10 μM compound (a). The compound alone showed some cell death at the 2 highest concentrations, 4.96 and 10 μM (b). Results are from 4 separate experiments and the error bars are SD.

Thirdly, compounds were assayed in a γH2AX foci assay which is a marker of DNA repair¹¹ (Figure 7). A delay in repair of γH2AX foci was observed after 6 hours post treatment of cells with cisplatin in combination with compound **13** as indicated by a right shift towards higher numbers of foci per cell.

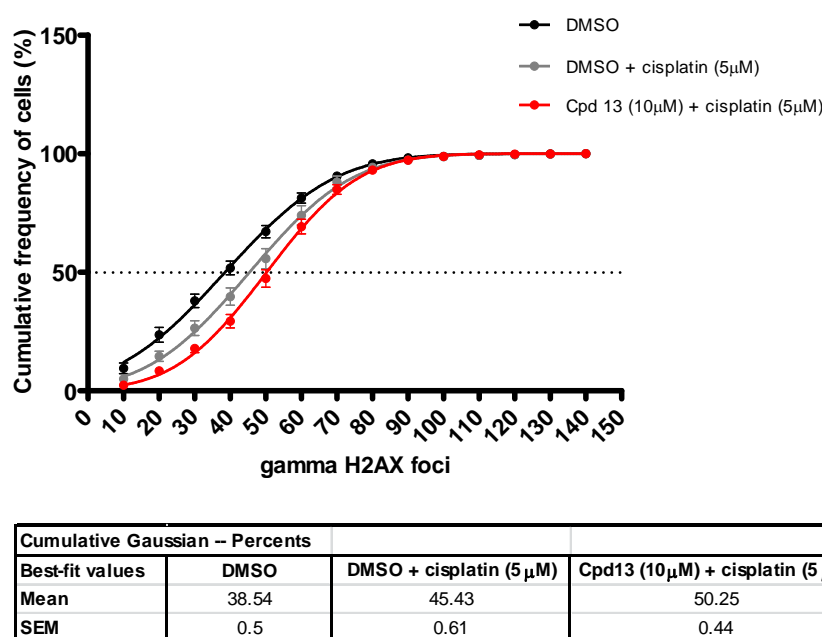


Figure 7. Compound **13** activity in a γH2AX foci imaging assay. γH2AX foci count in A375 cells pretreated with compound for 1h, exposed to 5 μM cisplatin for 1h and continued exposure to compound at 10 μM for 6h. Levels of γH2AX were quantified by immunofluorescence using a specific antibody (Millipore) and results analysed on an InCell 2000 High Content Imager (GE Healthcare). Relative cumulative frequency plots were used in order to visualize the shift in the response to cisplatin and compound treatment. Compound **13** causes a delay in DNA repair as illustrated by the rightward shift of the curve showing that cells contain larger numbers of foci. The combined treatment of cisplatin and compound **13** is significantly more than cisplatin alone ($p=0.0012$ by Sum of Squares F test of the EC_{50}). Results are from 2 representative experiments (triplicate tests in each) and the error bars are SEM.

In summary, we have shown that compounds containing a catechol or a 3-hydroxypyridone motif inhibited ERCC1-XPF with sub-micromolar or low micromolar potency in the endonuclease biochemical assay and displayed high selectivity over the other two nucleases tested. Exemplars from both series showed binding to ERCC1-XPF by SPR, and the leading example compound **13** showed inhibition of DNA repair in A375 melanoma cells across three assay formats. Further studies are required to understand the binding mode and cellular mechanism of action of these compounds.

Acknowledgements

The authors thank David Tickle, Sadhia Khan, Nathalie Bouloc and Zaynab Isseljee for *in vitro* ADMET and Martin Wear for production of ERCC1-XPF protein.

References and notes

1. McNeil, E. M.; Melton, D. W. *Nucleic Acids Res.* **2012**, *40*, 9990.
2. Jordheim, L. P.; Barakat, K. H.; Heinrich-Balard, L.; Matera, E. L.; Cros-Perrial, E.; Bouledrak, K.; El Sabeh, R.; Perez-Pineiro, R.; Wishart, D. S.; Cohen, R.; Tuszynski, J.; Dumontet, C. *Mol. Pharmacol.* **2013**, *84*, 12.
3. McNeil, E. M.; Ritchie, A. M.; Astell, K. R.; Shave, S.; Houston, D. R.; Bakrania, P.; Jones, H. M.; Khurana, P.; Wallace, C.; Chapman, T.; Wear, M. A.; Walkinshaw, M. D.; Saxty, B.; Melton, D. W. *DNA Repair* **2015**, *31*, 19.
4. Chen, E.; Swift, R. V.; Alderson, N.; Feher, V. A.; Feng, G. S.; Amaro, R. E. *ACS Med. Chem. Lett.* **2014**, *5*, 61.
5. Bauman, J. D.; Patel, D.; Baker, S. F.; Vijayan, R. S.; Xiang, A.; Parhi, A. K.; Martinez-Sobrido, L.; LaVoie, E. J.; Das, K.; Arnold, E. *ACS Chem. Biol.* **2013**, *8*, 2501.
6. Parhi, A. K.; Xiang, A.; Bauman, J. D.; Patel, D.; Vijayan, R. S.; Das, K.; Arnold, E.; Lavoie, E. J. *Bioorg. Med. Chem.* **2013**, *21*, 6435.
7. Baell, J. B.; Holloway, G. A. *J. Med. Chem.* **2010**, *53*, 2719.
8. Baell, J.; Walters, M. A. *Nature* **2014**, *513*, 481.
9. NER-GFP reporter assay: it should be noted that in this assay, the luciferase signal provides a control for transfection efficiency and for any non-NER-related effects of the compounds. For each compound concentration, the effect of the compound on NER was determined by dividing the GFP/luciferase ratio for the damaged GFP plasmid by the same ratio for the non-damaged GFP plasmid. This value was then divided by the equivalent value for control cultures without any compound and plotted as % NER activity (DNA Repair Index) against compound concentration to obtain the IC₅₀. Levels of repaired GFP expression can vary and, following normalization, larger error bars may be generated than in samples where GFP repair is reduced to very low and consistent levels by higher concentrations of active compound (see exemplar compound in Figure 5).
10. Cisplatin combination assay: compound activity was measured over a concentration range of 0.6–10 μ M for 5 days to assess potential shifts in potency of cell death caused by a dose response of cisplatin (0.1–3 μ M)
11. γ H2AX foci assay: A375 cells pre-treated with compound for 1h were exposed to 5 μ M cisplatin for 1h to induce DNA damage and therefore increase levels of γ H2AX foci. The cisplatin was removed and replaced with 1, 3 and 10 μ M compound. Cells were fixed with 4% paraformaldehyde 0, 17, 24 and 48h after cisplatin removal and processed for immunocytochemistry using a γ H2AX antibody (Millipore). The number of foci per cell was quantified using a high content imager (InCell 2000, GE Healthcare). Cell numbers containing 0-10, 10-20, 30-40 etc foci were binned and expressed as relative cumulative frequency.